PHYSICAL REVIEW D **91,** 074015 (2015)

Drell-Yan lepton pair production at NNLO QCD with parton showers

Stefan Höche,[1] Ye Li,[1] and Stefan Prestel[2]
[1]*SLAC National Accelerator Laboratory, Menlo Park, California 94025, USA*
[2]*Deutsches Elektronen-Synchrotron, DESY, 22603 Hamburg, Germany*
(Received 15 May 2014; published 13 April 2015)

We present a simple approach to combine NNLO QCD calculations and parton showers, based on the UNLOPS technique. We apply the method to the computation of Drell-Yan lepton-pair production at the Large Hadron Collider. We comment on possible improvements and intrinsic uncertainties.

DOI: 10.1103/PhysRevD.91.074015 PACS numbers: 12.38.Bx, 13.85.-t, 13.87.-a

I. INTRODUCTION

The combination of fully exclusive next-to-leading order (NLO) calculations in perturbative quantum chromodynamics with resummed predictions from parton showers has been in the focus of interest for the past decade. A wide range of matching [1–5] and merging [6–13] methods has been developed and implemented in Monte Carlo event generators [14]. By now they are standard tools for simulating final states at hadron colliders such as the LHC. However, so far only three proposals were made that extend these methods to next-to-next-to-leading order (NNLO) in the strong coupling expansion [8,15,16], and only two of them were implemented. They allow NNLO accurate particle-level simulations of two-jet production at LEP [8] and Higgs production via gluon fusion at hadron colliders [15]. Event generators for Drell-Yan lepton pair production at NNLO QCD matched to parton showers are not available. Due to the high relevance of this process as a standard candle for the LHC and possible future hadron colliders, we address the problem in this article, and we also provide a simple formulation for matching at NNLO, improving upon the UNLOPS method suggested in [10]. We use the Monte Carlo event generator SHERPA [17], including a parton shower [18] based on Catani-Seymour dipole subtraction [19], combined with the BlackHat library [20] for one-loop matrix elements. This implementation is publicly available.

Our matching scheme, which we call UN^{2}LOPS, preserves both the logarithmic accuracy of the parton shower and the fixed-order accuracy of the NNLO calculation.[1] It is a generic method to augment NNLO calculations with the primitive resummation encoded in an existing parton shower. At NLO, a considerable difference exists between matching methods, pertaining to the treatment of the finite remainder of higher-order corrections. This difference must be reduced at NNLO. The excellent convergence of the perturbative series in the Drell-Yan process further reduces potential differences. We therefore expect that UN^{2}LOPS will serve as a useful benchmark for future, more sophisticated NNLO matching schemes. The parton shower employed in our calculations already includes full color and spin information in the first emission term and the associated Sudakov factor [4]. It is therefore improved compared to the standard large-N_c approximation with spin averaging.

The outline of this article is as follows: Sec. II gives an introduction to the problem of matching at NLO and outlines our simplified approach. Section III extends the simplified UNLOPS method to NNLO, which we dub UN^{2}LOPS. Section IV contains first results from applying the method to Drell-Yan lepton pair production at the LHC. We also present some benchmark results for a high-energy LHC and a possible future proton-proton collider at 100 TeV center-of-mass energy. Section V contains some concluding remarks.

II. A SIMPLE EXAMPLE

To set the stage for the discussion of our method at NNLO we reformulate in this section the UNLOPS method and simplify its event generation algorithm. The extension to NNLO is then nearly straightforward. It will be presented in Sec. III.

The leading-order expression for an observable O is written as

$$\langle O\rangle^{(\mathrm{LO})} = \int \mathrm{d}\Phi_0 \mathrm{B}_0(\Phi_0) O(\Phi_0), \tag{1}$$

where Φ_0 is the differential Born phase-space element, and $\mathrm{B}_0(\Phi_0)$ is the Born differential cross section, including symmetry and flux factors as well as parton luminosities. We now add and subtract Sudakov-reweighted real-emission tree-level cross sections, denoted by B_1 [7]:

[1]For the purpose of this article, we assume that the parton shower is next-to-leading logarithmic (NLL) accurate, by including all effects described in [21]. Color coherence is implemented through dipole splitting operators rather than angular ordering. By maintaining the parton shower accuracy in the matching we mean preserving the logarithmic structure up to NLL in the Sudakov exponent as well as local four-momentum conservation as given by the shower kinematics.

$$\left[\int \mathrm{d}\Phi_0 \mathrm{B}_0(\Phi_0) O(\Phi_0) - \int_{t_c} \mathrm{d}\Phi_1 \Pi_0(t_1,\mu_Q^2)\mathrm{B}_1(\Phi_1) O(\Phi_0)\right] + \int_{t_c} \mathrm{d}\Phi_1 \Pi_0(t_1,\mu_Q^2)\mathrm{B}_1(\Phi_1) O(\Phi_1). \quad (2)$$

To the accuracy of the parton shower, this method is equivalent to the modified subtraction in MC@NLO [1] and POWHEG [2], as discussed at the end of this section. In the second term in the square bracket, the observable O is taken at the reduced phase-space point, determined by clustering the one-parton state Φ_1 to Φ_0 using an algorithm that corresponds to inverting the parton shower [22]. In other words, both terms in the square bracket enter the prediction for O with Born kinematics, while the last term enters with real-emission kinematics. This method is called a modified NLO subtraction scheme [1].

We have defined the parton shower no-branching probability for an n-parton state,

$$\Pi_n(t,t';\Phi_n) = \exp\left\{-\int_t^{t'} \mathrm{d}\hat{\Phi}_1 \mathrm{K}_n(\Phi_n,\hat{\Phi}_1)\right\}, \quad (3)$$

where K_n is the sum of differential branching probabilities, including luminosity and flux factors for initial-state evolution as appropriate [23]. In the case of Dokshitzer-Gribov-Lipatov-Altarelli-Parisi evolution, we have [14,24]

$$\mathrm{K}_n(\Phi_n,\hat{\Phi}_1) = \sum_{i=1}^{n_{\mathrm{in}}} \sum_{b=q,g} \frac{\alpha_s}{2\pi} P_{a_i b}(z) \frac{f_b(x_i/z,t)}{z f_{a_i}(x_i,t)} \Theta(z-x_i) + \sum_{i=n_{\mathrm{in}}+1}^{n_{\mathrm{in}}+n_{\mathrm{out}}} \sum_{b=q,g} \frac{\alpha_s}{2\pi} P_{a_i b}(z). \quad (4)$$

Note that K_n depends on Φ_n through the Bjorken variables x_i. The multiparticle phase-space elements factorize as $\mathrm{d}\Phi_{n+1} = \mathrm{d}\Phi_n \mathrm{d}\hat{\Phi}_1$, with $\mathrm{d}\hat{\Phi}_1$ the phase-space element for the emission of a single additional parton. We can write $\mathrm{d}\hat{\Phi}_1 = \mathrm{d}t\mathrm{d}z\mathrm{d}\phi/(2\pi) J(t,z,\phi)$, where t is the evolution variable of the parton shower, z is the splitting variable, and J is a Jacobian factor. t_c denotes the infrared cutoff, and μ_Q^2 is the resummation scale. Note that the parton shower employed here covers the full emission phase space, except for the region $t < t_c$. For ease of notation we have defined $t_1 = t(\Phi_1)$.

Equation (2) describes the one-parton state in the simplest possible matching approach. We can use the unitarity constraint on the parton shower,

$$\Pi_0(t_c,\mu_Q^2) = 1 - \int_{t_c} \mathrm{d}\Phi_1 \mathrm{K}_0(\hat{\Phi}_1)\Pi_0(t_1,\mu_Q^2), \quad (5)$$

to rearrange the terms depending on $O(\Phi_0)$:

$$\begin{aligned}&\int \mathrm{d}\Phi_0 \mathrm{B}_0(\Phi_0) O(\Phi_0) - \int_{t_c} \mathrm{d}\Phi_1 \Pi_0(t_1,\mu_Q^2)\mathrm{B}_1(\Phi_1) O(\Phi_0)\\ &= \int \mathrm{d}\Phi_0 \mathrm{B}_0(\Phi_0)\Pi_0(t_c,\mu_Q^2) O(\Phi_0)\\ &\quad - \int_{t_c} \mathrm{d}\Phi_1 \Pi_0(t_1,\mu_Q^2)[\mathrm{B}_1(\Phi_1)\\ &\quad - \mathrm{B}_0(\Phi_0)\mathrm{K}_0(\Phi_0,\hat{\Phi}_1)] O(\Phi_0). \end{aligned} \quad (6)$$

The term in square brackets is not logarithmically enhanced, as $\mathrm{B}_1 \to \mathrm{B}_0\mathrm{K}_0$ in the infrared limit. Therefore, Eq. (2) reproduces the parton shower resummation. At the same time, using B_1 instead of $\mathrm{B}_0\mathrm{K}_0$ does not affect the differential cross section as a function of the Born kinematics, Φ_0.

Additional emissions can be generated by replacing $O(\Phi_1)$ with the parton shower generating functional $\mathcal{F}_1(t_1,O)$, where

$$\begin{aligned}&\mathcal{F}_n(t,O) = \Pi_n(t_c,t) O(\Phi_n)\\ &\qquad + \int_{t_c}^{t} \mathrm{d}\hat{\Phi}_1 \mathrm{K}_n(\hat{\Phi}_1)\Pi_n(\hat{t},t)\mathcal{F}_{n+1}(\hat{t},O),\\ &\text{where } \hat{t} = t(\hat{\Phi}_1). \end{aligned} \quad (7)$$

We now replace the Born differential cross section in Eq. (2) by the differential NLO cross section

$$\bar{\mathrm{B}}(\Phi_0) = \mathrm{B}_0(\Phi_0) + \tilde{\mathrm{V}}_0(\Phi_0) + \mathrm{I}_0(\Phi_0) + \int \mathrm{d}\hat{\Phi}_1 [\mathrm{B}_1(\Phi_0,\hat{\Phi}_1) - \mathrm{S}_0(\Phi_0,\hat{\Phi}_1)]. \quad (8)$$

$\tilde{\mathrm{V}}_0$ denotes the UV finite part of the virtual corrections, including collinear mass factorization counterterms, I_0 are integrated NLO subtraction terms [19], and S_0 the corresponding real subtraction terms. The matched result is given by

$$\left\{\int \mathrm{d}\Phi_0 \bar{\mathrm{B}}_0^{t_c}(\Phi_0) + \int_{t_c} \mathrm{d}\Phi_1 [1-\Pi_0(t_1,\mu_Q^2)]\mathrm{B}_1(\Phi_1)\right\} O(\Phi_0) + \int_{t_c} \mathrm{d}\Phi_1 \Pi_0(t_1,\mu_Q^2)\mathrm{B}_1(\Phi_1)\mathcal{F}_1(t_1,O), \quad (9)$$

where we have defined the vetoed cross section

$$\bar{\mathrm{B}}_0^{t_c}(\Phi_0) = \bar{\mathrm{B}}_0(\Phi_0) - \int_{t_c} \mathrm{d}\hat{\Phi}_1 \mathrm{B}_1(\Phi_0,\hat{\Phi}_1). \quad (10)$$

Equation (9) already contains the essence of our method. The three terms can be generated in a Monte Carlo simulation as follows: $\bar{\mathrm{B}}_0^{t_c}$ is a fixed-order contribution, which does not undergo parton showering. B_1 is assigned a parton shower "history" using the clustering procedure first proposed in [22]. The zero-parton state defined in this clustering undergoes truncated parton shower evolution. By definition,

the survival probability is $\Pi_0(t_1,\mu_Q^2)$, while the corresponding branching probability is $1-\Pi_0(t_1,\mu_Q^2)$. Thus, if an emission is generated, the event is kept in the selected zero-parton state, as indicated by the observable dependence $O(\Phi_0)$ in the first term of Eq. (9). If no emission is generated, the event undergoes parton showering, starting from the one-parton state. This procedure is an improvement of UNLOPS and ensures that no counter-events with negative weights must be generated during the matching.

Up to now we have ignored renormalization and factorization scale dependence in B_1. While terms generated by the running of the strong coupling are formally of higher order and therefore do not modify the fixed-order accuracy of the matched result, they are important to restoring the logarithmic accuracy of the parton shower. The same reasoning applies to scaling violations in the parton distribution functions (PDFs). Scales can be adjusted to their parton shower values by reweighting, eventually leading to the improved UNLOPS matching formula

$$\begin{aligned}\langle O\rangle^{(\mathrm{UNLOPS})} &= \left\{\int \mathrm{d}\Phi_0 \bar{\mathrm{B}}_0^{t_c}(\Phi_0) \right. \\ &\quad \left. + \int_{t_c} \mathrm{d}\Phi_1 [1-\Pi_0(t_1,\mu_Q^2) w_1(\Phi_1)]\mathrm{B}_1(\Phi_1)\right\} O(\Phi_0) \\ &\quad + \int_{t_c} \mathrm{d}\Phi_1 \Pi_0(t_1,\mu_Q^2) w_1(\Phi_1)\mathrm{B}_1(\Phi_1)\mathcal{F}_1(t_1,O). \end{aligned} \tag{11}$$

In the case of Drell-Yan lepton pair production we need to match a single initial-state parton splitting $a\to\{a',j\}$. The weight $w_1(\Phi_1)$ is then defined as [10]

$$w_1(\Phi_1) = \frac{\alpha_s(bt_1)}{\alpha_s(\mu_R^2)}\frac{f_a(x_a,t_1)}{f_a(x_a,\mu_F^2)}\frac{f_{a'}(x_{a'},\mu_F^2)}{f_{a'}(x_{a'},t_1)}$$
$$\text{where } \beta_0 \ln\frac{1}{b} = \left(\frac{67}{18}-\frac{\pi^2}{6}\right)C_A - \frac{10}{9}T_R n_f. \tag{12}$$

$f_a(x_a)$ and $f_{a'}(x_{a'})$ denote the PDFs associated with the external and intermediate parton, respectively. The scale factor b includes effects of the two-loop cusp anomalous dimension in the parton shower [21].

The event generation procedure is modified as follows: Weights of one-jet events are multiplied by $1+2|w_1-1|$. In a fraction $1/(2+1/|w_1-1|)$, the event is weighted by $\mathrm{sgn}(w_1-1)$, and the point is discarded if an emission is generated in the truncated parton shower. If the event is kept, it is reduced to Born kinematics and the sign of its weight inverted with probability $1/2$. This procedure sums—in a Monte Carlo fashion—over two event types, which either contain factors of Π_0 or $1-\Pi_0$, or else the terms $\pm\Pi_0(w_1-1)$. This can lead again to the generation of negative weights, however their fraction is much reduced compared to the original UNLOPS scheme.

Equation (11) still holds if the phase-space separation is not achieved in terms of the parton shower evolution parameter, i.e. if the integration boundaries for $\bar{\mathrm{B}}_0^{t_c}$ and $\int_{t_c}\mathrm{d}\Phi_1\mathrm{B}_1$ are not given by t_c. In this case, one can split the real-emission contribution into a pure fixed-order part and a contribution where parton shower resummation is applied. In the following, we therefore define $\Pi_n(t,t') = \Pi_n(t_c,t')$ for all $t<t_c$.

We conclude this section with a comparison to the POWHEG method [2]. Assuming that the parton shower evolution kernels for the first emission can be replaced by $\mathrm{K}_0\to\bar{\mathrm{K}}_0 = w_1\mathrm{B}_1/\mathrm{B}_0$, we obtain from Eq. (11)

$$\begin{aligned}\langle O\rangle^{(\mathrm{UNLOPS})} \to &\int \mathrm{d}\Phi_0 \mathrm{B}_0(\Phi_0)\bar{\mathcal{F}}_0(\mu_Q^2,O) \\ &+ \int \mathrm{d}\Phi_0[\bar{\mathrm{B}}_0(\Phi_0)-\mathrm{B}_0(\Phi_0)]O(\Phi_0). \end{aligned} \tag{13}$$

The main difference compared to the POWHEG result,

$$\langle O\rangle^{(\mathrm{POWHEG})} = \int \mathrm{d}\Phi_0 \bar{\mathrm{B}}_0(\Phi_0)\bar{\mathcal{F}}_0(\mu_Q^2,O), \tag{14}$$

is that the finite remainder of higher-order corrections (after UV renormalization and IR subtraction), $\bar{\mathrm{B}}_0-\mathrm{B}_0$, does not undergo parton showering in UNLOPS, while it does in POWHEG. A comparison with MC@NLO leads to the same conclusion. While it is not obvious from the matching conditions at NLO, whether UNLOPS or POWHEG is the more natural prescription, the NNLO matching conditions require that UNLOPS at NNLO behaves identically to both MC@NLO and POWHEG in this regard, i.e. that the finite remainder multiplies, $\mathcal{F}_0(\mu_Q^2,O)$, rather than $O(\Phi_0)$. We will return to this question at the end of Sec. III.

III. UN^{2}LOPS WITH PHASE-SPACE SLICING

We first describe our calculation of the NNLO vetoed cross section, corresponding to Eq. (10). It is performed in the q_T cutoff method, based on the ideas of q_T subtraction [25]. All soft and collinear singularities of NNLO origin cancel within the zero-q_T bin, leading to a finite differential cross section, $\bar{\mathrm{B}}_0^{=q_{T,\mathrm{cut}}}$. The remainder is computed as an NLO result for the original Born process plus one additional jet.

The NNLO cross section with a small cut on observables like q_T of the gauge boson has a simple factorization formula, which can be described up to power corrections in the cutoff, $q_{T,\mathrm{cut}}$, by effective field theory. This form is generally more compact than the full NNLO result. The cutoff method has been used previously to compute top decays fully exclusively at NNLO [26]. We adopt the framework developed in [27] to obtain the vetoed cross section. All components needed for two-loop results for the Drell-Yan process have recently been computed [28], and verified against the hard collinear coefficients [29] used by the original q_T subtraction method.

The contribution at $q_T > q_{T,\mathrm{cut}}$ is computed as a standard NLO QCD result, using Catani-Seymour dipole subtraction to regularize infrared divergences [19]. This type of calculation has been fully automated [30]. We use SHERPA [17,31] for tree-level-like contributions and BlackHat [20] for virtual corrections. We match this computation to the parton shower using a variant of the MC@NLO method, which is described in [4]. The corresponding expression for the $q_T > q_{T,\mathrm{cut}}$ cross section depending on an infrared-safe observable O is

$$\langle O\rangle^{(\mathrm{NLO})}_{>q_{T,\mathrm{cut}}} = \int_{q_{T,\mathrm{cut}}} \mathrm{d}\Phi_1 \tilde{\mathrm{B}}_1(\Phi_1)\tilde{\mathcal{F}}_1(t_1,O) + \int_{q_{T,\mathrm{cut}}} \mathrm{d}\Phi_2 \mathrm{H}_1(\Phi_2)\mathcal{F}_2(t_2,O), \tag{15}$$

where the one-jet differential NLO cross section and the hard remainder are defined as

$$\begin{aligned}\tilde{\mathrm{B}}_1(\Phi_1) &= \mathrm{B}_1(\Phi_1) + \tilde{\mathrm{V}}_1(\Phi_1) + \mathrm{I}_1(\Phi_1) \\ &\quad - \int_{t_c} \mathrm{d}\hat{\Phi}_1 \mathrm{S}_1(\Phi_1,\hat{\Phi}_1)\Theta(t_2(\hat{\Phi}_1) - t_1(\Phi_1)), \\ \mathrm{H}_1(\Phi_2) &= \mathrm{B}_2(\Phi_2) - \mathrm{S}_1(\Phi_2)\Theta(t_1(\Phi_2) - t_2(\Phi_2)).\end{aligned} \tag{16}$$

The generating functional of the MC@NLO is

$$\tilde{\mathcal{F}}_1(t,O) = \tilde{\Pi}_1(t_c,t_1)O(\Phi_1) + \int_{t_c} \mathrm{d}\hat{\Phi}_1 \frac{\mathrm{S}_1(\Phi_1,\hat{\Phi}_1)}{\mathrm{B}_1(\Phi_1)} \tilde{\Pi}_1(\hat{t},t_1)\mathcal{F}_2(\hat{t},O), \tag{17}$$

with the no-branching probability given by parton shower unitarity:

$$\tilde{\Pi}_1(t,t',\Phi_n) = \exp\left\{-\int_t^{t'} \mathrm{d}\hat{\Phi}_1 \frac{\mathrm{S}_1(\Phi_1,\hat{\Phi}_1)}{\mathrm{B}_1(\Phi_1)}\right\}. \tag{18}$$

Note that we choose $q_{T,\mathrm{cut}} \leq 1$ GeV, which is below the cutoff of the initial-state parton shower.

Equation (15) produces the correct dependence on the observable O at next-to-leading QCD for $q_T > q_{T,\mathrm{cut}}$. It can thus be used to complement the exclusive NNLO calculation in the zero-q_T bin. However, the two calculations cannot be naively added as in Eq. (11), since this would spoil the $\mathcal{O}(\alpha_s^2)$ accuracy of the full result. This problem was also addressed by NLO merging methods [8–11], and by the MINLO scale setting procedure [32]. The $\mathcal{O}(\alpha_s)$ contribution to the fixed-order expansion of the parton shower must first be subtracted, which can be achieved efficiently by omitting the first emission in a truncated shower [9], or by explicit subtraction [8,10]. Correspondingly, any $\mathcal{O}(\alpha_s)$ contribution must be subtracted from the corrective weight, Eq. (12). The full formula describing our combination method can be written as

$$\begin{aligned}\langle O\rangle^{(\mathrm{UN^2LOPS})} &= \int \mathrm{d}\Phi_0 \bar{\bar{\mathrm{B}}}_0^{q_{T,\mathrm{cut}}}(\Phi_0)O(\Phi_0) \\ &\quad + \int_{q_{T,\mathrm{cut}}} \mathrm{d}\Phi_1 [1-\Pi_0(t_1,\mu_Q^2)(w_1(\Phi_1) + w_1^{(1)}(\Phi_1) + \Pi_0^{(1)}(t_1,\mu_Q^2))]\mathrm{B}_1(\Phi_1)O(\Phi_0) \\ &\quad + \int_{q_{T,\mathrm{cut}}} \mathrm{d}\Phi_1 \Pi_0(t_1,\mu_Q^2)(w_1(\Phi_1) + w_1^{(1)}(\Phi_1) + \Pi_0^{(1)}(t_1,\mu_Q^2))\mathrm{B}_1(\Phi_1)\bar{\mathcal{F}}_1(t_1,O) \\ &\quad + \int_{q_{T,\mathrm{cut}}} \mathrm{d}\Phi_1 [1-\Pi_0(t_1,\mu_Q^2)]\tilde{\mathrm{B}}_1^{\mathrm{R}}(\Phi_1)O(\Phi_0) + \int_{q_{T,\mathrm{cut}}} \mathrm{d}\Phi_1 \Pi_0(t_1,\mu_Q^2)\tilde{\mathrm{B}}_1^{\mathrm{R}}(\Phi_1)\bar{\mathcal{F}}_1(t_1,O) \\ &\quad + \int_{q_{T,\mathrm{cut}}} \mathrm{d}\Phi_2 [1-\Pi_0(t_1,\mu_Q^2)]\mathrm{H}_1^{\mathrm{R}}(\Phi_2)O(\Phi_0) + \int_{q_{T,\mathrm{cut}}} \mathrm{d}\Phi_2 \Pi_0(t_1,\mu_Q^2)\mathrm{H}_1^{\mathrm{R}}(\Phi_2)\mathcal{F}_2(t_2,O) \\ &\quad + \int_{q_{T,\mathrm{cut}}} \mathrm{d}\Phi_2 \mathrm{H}_1^{\mathrm{E}}(\Phi_2)\mathcal{F}_2(t_2,O).\end{aligned} \tag{19}$$

We have defined $\tilde{\mathrm{B}}^{\mathrm{R}} = \tilde{\mathrm{B}} - \mathrm{B}$ and the regular and exceptional part of the hard remainder

$$\begin{aligned}\mathrm{H}_1^{\mathrm{R}}(\Phi_2) &= \mathrm{H}_1(\Phi_2)\Theta(t_1-t_2)\Theta(t_2-t_c), \\ \mathrm{H}_1^{\mathrm{E}}(\Phi_2) &= \mathrm{H}_1(\Phi_2) - \mathrm{H}_1^{\mathrm{R}}(\Phi_2).\end{aligned} \tag{20}$$

The exceptional contributions $\mathrm{H}_1^{\mathrm{E}}$ contain phase-space regions for which no ordered parton shower history can be identified, as well as two-parton states that do not allow an interpretation as having evolved from a zero- or one-parton state via QCD-type parton splittings. Exceptional contributions do not undergo the truncated parton showering used to produce $\Pi_0(t_1,\mu_Q^2)$, as they do not generate

logarithmic corrections at parton shower accuracy. Ambiguities in the matched result due to exceptional configurations will be important for matching at higher logarithmic accuracy, and can be resolved as soon as the parton shower is amended with the necessary subleading logarithmic corrections and electroweak splittings. This will allow us to treat such states in the same manner as the regular configurations.

The subtraction terms for the no-branching probability of the parton shower, and for the weight w_1, are given by

$$\Pi_0^{(1)}(t,t') = \int_t^{t'} \mathrm{d}\hat{\Phi}_1 \frac{\alpha_s(\mu_R^2)}{\alpha_s(b\hat{t})} \mathrm{K}_1(\Phi_1,\hat{\Phi}_1)$$
$$w_1^{(1)}(\Phi_1) = \frac{\alpha_s(\mu_R^2)}{2\pi}\left[\beta_0 \log\frac{bt_1}{\mu_R^2} - \log\frac{t_1}{\mu_F^2}\sum_c\left(\int_x^1 \frac{\mathrm{d}z}{z} P_{ca}(z)\frac{f_c(x/z,\mu_F^2)}{f_a(x,\mu_F^2)} - \int_{x'}^1 \frac{\mathrm{d}z}{z} P_{ca'}(z)\frac{f_c(x'/z,\mu_F^2)}{f_{a'}(x',\mu_F^2)}\right)\right]. \quad (21)$$

They are generated by the Monte Carlo procedure outlined below Eq. (12). Note that $1-\Pi_0(w_1+w_1^{(1)}+\Pi_0^{(1)})$ is of order α_s^2. Therefore, it is easy to see that the method does not spoil the accuracy of the fixed-order calculation. To investigate whether the logarithmic accuracy of the parton shower resummation is maintained, we take the collinear limit, $t_1 \to 0$. In this limit, $\mathrm{H}_1^{\mathrm{E}}$ only generates logarithms that are beyond the parton shower approximation, and it can thus be ignored. Consequently, for $q_T > q_{T,\mathrm{cut}}$, we are left with

$$\int_{q_{T,\mathrm{cut}}} \mathrm{d}\Phi_1 \Pi_0(t_1,\mu_Q^2) w_1(\Phi_1)\mathrm{B}_1(\Phi_1)\bar{\mathcal{F}}_1(t_1,O) + \int_{q_{T,\mathrm{cut}}} \mathrm{d}\Phi_1 \Pi_0(t_1,\mu_Q^2)\mathrm{R}_1(\Phi_1,O) \quad (22)$$

where

$$\mathrm{R}_1(\Phi_1,O) = (\mathrm{B}_1(\Phi_1)(w_1^{(1)}(\Phi_1)+\Pi_0^{(1)}(t_1,\mu_Q^2)) + \tilde{\mathrm{B}}_1^{\mathrm{R}}(\Phi_1))\bar{\mathcal{F}}_1(t_1,O) + \int \mathrm{d}\hat{\Phi}_1 \mathrm{H}_1^{\mathrm{R}}(\Phi_1,\hat{\Phi}_1)\mathcal{F}_2(t_2,O). \quad (23)$$

The first term in Eq. (22) is, to the required accuracy, equivalent to the parton shower result. Thus it remains to be shown that R_1 contains only subleading terms. In the soft and collinear limit, $\mathrm{H}_1^{\mathrm{R}}$ does not contribute at the required accuracy [1]. Quark propagators in $\tilde{\mathrm{B}}_1^{\mathrm{R}}$ can to first order be approximated as $(1-\Pi_0^{(1)}(t,\mu_Q^2)-w_1^{(1)}+\alpha_s/(2\pi)\beta_0\log(bt/\mu_R^2))/\not{p}$ [33], where p is the quark momentum. Coupling renormalization leads to corrections of the form $\alpha_s/(2\pi)\beta_0\log(t/\mu_R^2)$, where t is the relative transverse momentum in the gluon emission [34]. The two-loop cusp anomalous dimension, simulated by means of the scale factor b in Eq. (12), is naturally present in $\tilde{\mathrm{B}}_1^{\mathrm{R}}$. The subtraction terms, Eq. (21), thus cancel all universal NLO corrections in $\tilde{\mathrm{B}}_1^{\mathrm{R}}$, which have already been included in the parton shower. The remainder is beyond the required accuracy. Using the unitarity condition for parton shower evolution, this argument extends to the region $q_T < q_{T,\mathrm{cut}}$. Note that because of the unitarity condition, also no spurious logarithms are generated in the inclusive cross section, and the NNLO accuracy is maintained exactly.

We now return to the difference between UNLOPS and POWHEG/MC@NLO discussed in Sec. II. When performing a one-jet matched NLO calculation in the UNLOPS implementation of [10], the nonuniversal terms in the first part of Eq. (23) do not undergo parton showering above the merging scale. The UN^{2}LOPS prescription instead introduces parton shower corrections to these terms throughout the real-emission phase space, and it includes a Sudakov form factor for a truncated shower to resum effects of unresolved emissions above the scale of the hard jet. This new matching condition is justified if we view the parton shower as an all-order calculation dressing a hard input state, which has a fixed-order expansion by itself, with the effects of soft and collinear radiation.[2] It can also be understood in the following way: In the collinear limit, the factorization of one-loop matrix elements leads to virtual corrections of the form $\mathrm{V}_0\mathrm{K}_0 + \mathrm{B}_0\mathrm{K}_0^{(1)}$, where $\mathrm{K}_0^{(1)}$ are the one-loop splitting kernels. When including the respective integrated subtraction terms and no-branching probabilities of the truncated parton shower, the remainder of the first term turns into $(\bar{\mathrm{B}}_0-\mathrm{B}_0)\mathrm{K}_0\Pi_0$, and can be interpreted as a parton shower combined with the finite remainder of the NLO corrections in the zero-q_T bin. This eliminates the difference between Eqs. (14) and (13).

Following this argument, one may conclude that the finite $\mathcal{O}(\alpha_s^2)$ corrections contained in zero-q_T configurations of Eq. (19) should also be "spread" across the one-parton (and two-parton) phase space by the parton shower, provided that the resulting change of the radiation pattern is at most $\mathcal{O}(\alpha_s^3)$. The difference between including and not

[2] A similar interpretation holds for factorization formulas in analytic resummation, for which a fixed-order hard function is convoluted with all-order soft and collinear functions, see for example [27] and [35].

TABLE I. Total cross sections for 60 GeV $\leq m_{ll} \leq$ 120 GeV at varying center-of-mass energy for a pp collider. Uncertainties from scale variations are given as sub-/superscripts. Statistical uncertainties from Monte Carlo integration are quoted in parentheses.

E_{cms}	7 TeV	14 TeV	33 TeV	100 TeV
VRAP	$973.99(9)^{+4.70}_{-1.84}$ pb	$2079.0(3)^{+14.7}_{-6.9}$ pb	$4909.7(8)^{+45.1}_{-27.2}$ pb	$13346(3)^{+129}_{-111}$ pb
SHERPA	$973.7(3)^{+4.78}_{-2.21}$ pb	$2078.2(10)^{+15.0}_{-8.0}$ pb	$4905.9(28)^{+45.1}_{-27.9}$ pb	$13340(14)^{+152}_{-110}$ pb

including such parton shower corrections is within the intrinsic uncertainty of NNLO matching schemes. We see no strong reason for implementing them in the simulation of the Drell-Yan process, due to the excellent convergence of the perturbative series. The assessment may differ in other reactions, like Higgs-boson production via gluon fusion, where higher-order corrections are large.

IV. RESULTS

This section presents results using an implementation of the UN^{2}LOPS algorithm in the event generator SHERPA [17]. We use a parton shower [18] based on Catani-Seymour dipole subtraction [19]. NLO virtual corrections for the one-jet process are provided by the BlackHat library [20]. Dipole subtraction is performed using AMEGIC [31,36]. For comparison to experimental data we use RIVET [37]. We use the Martin-Stirling-Thorne-Watt 2008 PDF set [38] and the corresponding definition of the running coupling. We work in the five flavor scheme. Electroweak parameters are given in the G_μ scheme as $m_Z = 91.1876\,\mathrm{GeV}$, $\Gamma_Z = 2.4952\,\mathrm{GeV}$, $m_W = 80.385\,\mathrm{GeV}$, $\Gamma_W = 2.085$ GeV, and $G_F = 1.1663787 \times 10^{-5}$ GeV^{-2}.

In order to cross-check our implementation we first compare the total cross section in the mass range 60 GeV $\leq m_{ll} \leq$ 120 GeV to results obtained from VRAP [39]. Table I shows that the predictions agree within the per-mill-level statistical uncertainty of the Monte Carlo integration. We also compared the central values to results from DYNNLO [25] and found full agreement. Additionally, we have checked that our predictions are identical when varying $q_{T,\mathrm{cut}}$ between 0.1 and 1 GeV. The default value is $q_{T,\mathrm{cut}} = 1$ GeV. Figure 1 compares differential cross sections from FEWZ [40] and SHERPA for the rapidity and invariant mass spectra of the Drell-Yan lepton pair. We computed the NLO reference results using NNLO PDFs. This is indicated in the figure by the label NLO′. It is interesting to observe the excellent agreement with the genuine NNLO predictions.

Figure 2 shows predictions from the matched calculation. We now include a simulation of higher-order QED corrections [41]. It is interesting to compare the matched prediction to the fixed-order NNLO result for the transverse momentum spectrum of the electron. In the region $p_{T,e} <$ 45 GeV the result is generically NNLO correct, while for $p_{T,e} >$ 45 GeV, it is effectively only NLO correct.

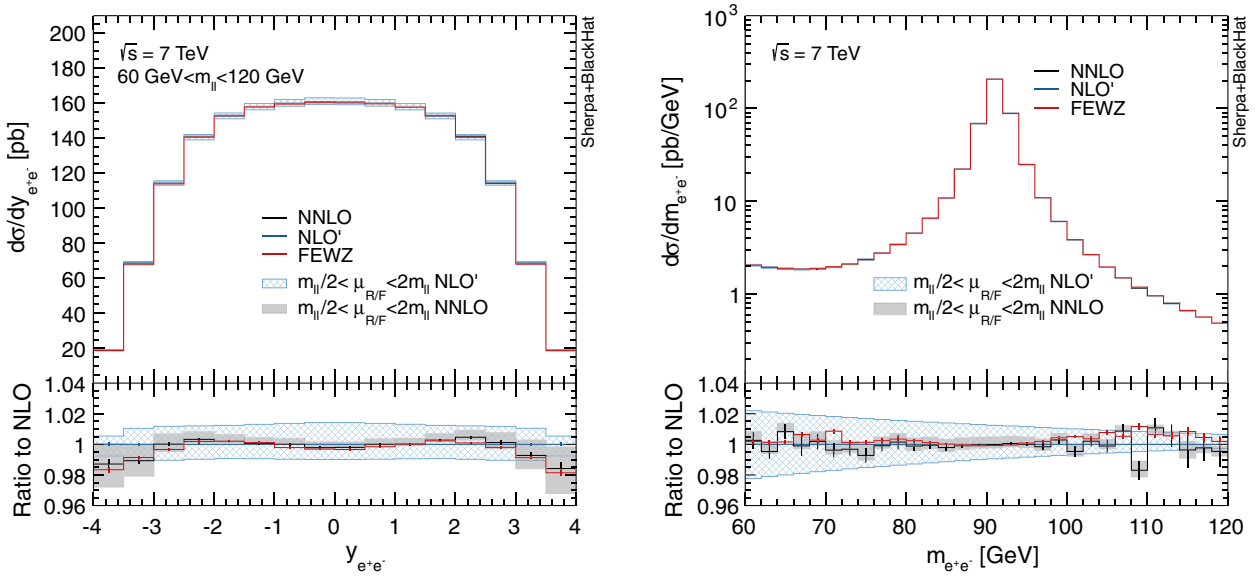

FIG. 1 (color online). Comparison between FEWZ and SHERPA for rapidity and invariant mass spectra of the Drell-Yan lepton pair. The gray solid (blue hatched) band shows scale uncertainties associated with the NNLO (NLO) prediction, obtained by varying $\mu_{R/F}$ in the range $m_{ll}/2 \leq \mu \leq 2m_{ll}$.

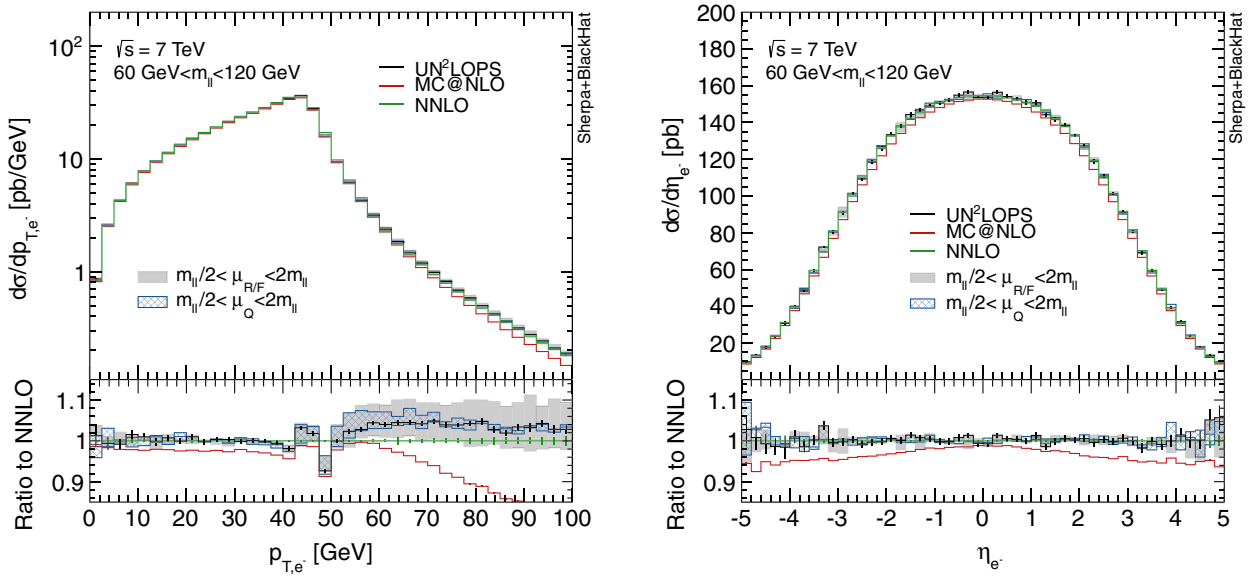

FIG. 2 (color online). Transverse momentum and rapidity spectrum of the electron. The gray solid (blue hatched) band shows scale uncertainties obtained by varying $\mu_{R/F/Q}$ (μ_Q) in the range $m_{ll}/2 \le \mu \le 2m_{ll}$.

Correspondingly, the uncertainty band is larger at high transverse momentum. The fixed-order prediction lies well within the NNLO scale uncertainty of the matched result, except for the transition region $p_{T,e} \gtrsim 45$ GeV, where real-emission corrections play the dominant role.

Figure 3 compares the transverse momentum spectrum of the Drell-Yan lepton pair to data from the CMS [42] and ATLAS [43] collaborations. These measurements are insensitive to generic NNLO corrections, which are generated only in the zero-q_T bin in our approach. However, they probe the form of the Sudakov form factor as simulated by the matched calculation, and they are therefore useful to judge whether the radiation pattern of the parton shower is preserved. The results indicate that higher-logarithmic corrections originating in $\tilde{B}_1^R$ and H_1 are numerically small and do not spoil our prediction. Note that the parton shower parameters in the matched calculation have not been tuned to fit either of these distributions. The

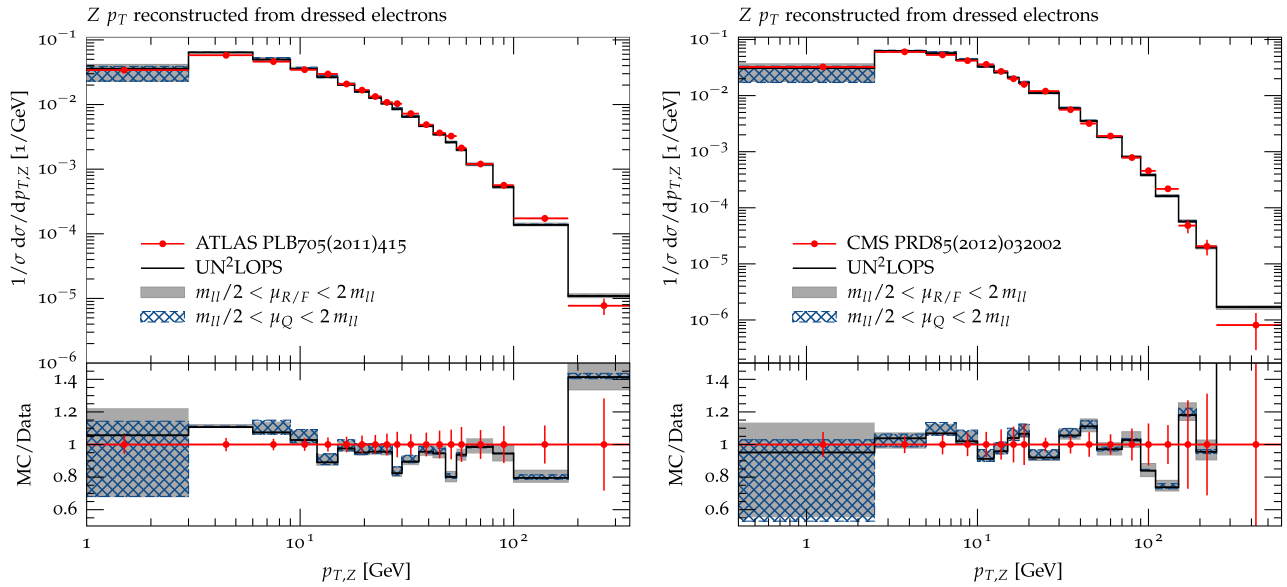

FIG. 3 (color online). UN^{2}LOPS prediction for the transverse momentum spectrum of the Drell-Yan lepton pair in comparison to ATLAS data from [43] (left panel) and CMS data from [42] (right panel). The gray solid (blue hatched) band shows scale uncertainties obtained by varying $\mu_{R/F/Q}$ (μ_Q) in the range $m_{ll}/2 \le \mu \le 2m_{ll}$.

large perturbative uncertainties in the first bin of both distributions do not lead to large uncertainties in the total cross section, but they indicate that higher-logarithmic resummation might be needed in order to improve the low-$p_{T,Z}$ region.

V. OUTLOOK

We have presented a simple method for matching NNLO calculations in perturbative QCD to existing parton showers, based on the UNLOPS technique. In contrast to the original implementation of UNLOPS, the event generation algorithm does not lead to large cancellations, and convergence of the Monte Carlo integration is much improved. Remaining uncertainties of the method are related to the treatment of finite remainders of the virtual corrections after UV renormalization and IR subtraction, and to the treatment of exceptional configurations in the hard remainder of double real corrections. Our method can be applied to arbitrary processes, and it can be systematically improved by using parton showers with higher logarithmic accuracy, which is currently an area of active research. The combination with higher-multiplicity NLO matched simulations is straightforward and can be achieved in both the UNLOPS [10] and MEPS@NLO [9] schemes.

We also provide an independent implementation of a fully differential NNLO calculation of Drell-Yan lepton pair production, using the q_T-cutoff method. Both the parton-level event generator and the shower-matched calculation are made publicly available in the framework of the SHERPA event generator. This also allows the production of Les Houches Event Files [44] or Ntuple files [45] containing NNLO event information at parton level.

ACKNOWLEDGMENTS

We are grateful to the BlackHat Collaboration for making the BlackHat library available for this study. We thank Lance Dixon, Frank Krauss, Leif Lönnblad, and HuaXing Zhu for helpful discussions and their comments on the manuscript. This work was supported by the U.S. Department of Energy under Contract No. DE-AC02-76SF00515. We used resources of the National Energy Research Scientific Computing Center, which is supported by the Office of Science of the U.S. Department of Energy under Contract No. DE-AC02-05CH11231.

[1] S. Frixione and B. R. Webber, J. High Energy Phys. 06 (2002) 029.
[2] P. Nason, J. High Energy Phys. 11 (2004) 040; S. Frixione, P. Nason, and C. Oleari*ibid.* 11 (2007) 070.
[3] K. Hamilton, P. Richardson, and J. Tully, J. High Energy Phys. 04 (2009) 116; P. Torrielli and S. Frixione*ibid.* 04 (2010) 110; S. Frixione, F. Stoeckli, P. Torrielli, and B. R. Webber*ibid.* 01 (2011) 053; S. Alioli, P. Nason, C. Oleari, and E. Re*ibid.* 06 (2010) 043; S. Höche, F. Krauss, M. Schönherr, and F. Siegert, *ibid.* 04 (2011) 024; R. Frederix, S. Frixione, V. Hirschi, F. Maltoni, R. Pittau, and P. Torrielli *ibid.* 02 (2012) 048; R. Frederix, S. Frixione, V. Hirschi, F. Maltoni, R. Pittau, and P. Torrielli*ibid.* 02 (2012) 099; S. Plätzer and S. Gieseke, Eur. Phys. J. C **72**, 2187 (2012).
[4] S. Höche, F. Krauss, M. Schönherr, and F. Siegert, J. High Energy Phys. 09 (2012) 049; Phys. Rev. Lett. **110**, 052001 (2013); S. Höche and M. Schönherr, Phys. Rev. D **86**, 094042 (2012).
[5] P. Nason and B. Webber, Annu. Rev. Nucl. Part. Sci. **62**, 187 (2012).
[6] S. Catani, F. Krauss, R. Kuhn, and B. R. Webber, J. High Energy Phys. 11 (2001) 063; L. Lönnblad, J. High Energy Phys. 05 (2002) 046; M. L. Mangano, M. Moretti, and R. Pittau, Nucl. Phys. **B632**, 343 (2002); F. Krauss, J. High Energy Phys. 08 (2002) 015; S. Höche, F. Krauss, S. Schumann, and F. Siegert, J. High Energy Phys. 05 (2009) 053; K. Hamilton, P. Richardson, and J. Tully, J. High Energy Phys. 11 (2009) 038; L. Lönnblad and S. Prestel, J. High Energy Phys. 03 (2012) 019.
[7] L. Lönnblad and S. Prestel, J. High Energy Phys. 02 (2013) 094.
[8] N. Lavesson and L. Lönnblad, J. High Energy Phys. 12 (2008) 070.
[9] T. Gehrmann, S. Höche, F. Krauss, M. Schönherr, and F. Siegert, J. High Energy Phys. 01 (2013) 144; S. Höche, F. Krauss, M. Schönherr, and F. Siegert, J. High Energy Phys. 04 (2013) 027.
[10] L. Lönnblad and S. Prestel, J. High Energy Phys. 03 (2013) 166.
[11] S. Plätzer, J. High Energy Phys. 08 (2013) 114.
[12] R. Frederix and S. Frixione, J. High Energy Phys. 12 (2012) 061.
[13] S. Alioli, C. W. Bauer, C. J. Berggren, A. Hornig, F. J. Tackmann, C. K. Vermilion, J. R. Walsh, and S. Zuberi, J. High Energy Phys. 09 (2013) 120.
[14] A. Buckley *et al.*, Phys. Rep. **504**, 145 (2011).
[15] K. Hamilton, P. Nason, E. Re, and G. Zanderighi, J. High Energy Phys. 10 (2013) 222.
[16] S. Alioli, C. W. Bauer, C. Berggren, F. J. Tackmann, J. R. Walsh, and S. Zuberi, J. High Energy Phys. 06 (2014) 089.
[17] T. Gleisberg, S. Höche, F. Krauss, A. Schälicke, S. Schumann, and J. Winter, J. High Energy Phys. 02 (2004) 056; T. Gleisberg, S. Höche, F. Krauss, M. Schönherr, S. Schumann, F. Siegert, and J. Winter, J. High Energy Phys. 02 (2009) 007.
[18] S. Schumann and F. Krauss, J. High Energy Phys. 03 (2008) 038.

[19] S. Catani and M. H. Seymour, Nucl. Phys. **B485**, 291 (1997); S. Catani, S. Dittmaier, M. H. Seymour, and Z. Trocsanyi, Nucl. Phys. **B627**, 189 (2002).
[20] C. F. Berger, Z. Bern, L. J. Dixon, F. Febres-Cordero, D. Forde, H. Ita, D. A. Kosower, and D. Maître, Phys. Rev. D **78**, 036003 (2008); C. F. Berger, Z. Bern, L. J. Dixon, F. Febres-Cordero, D. Forde, T. Gleisberg, H. Ita, D. A. Kosower, and D. Maître, Phys. Rev. D **80**, 074036 (2009); **82**, 074002 (2010); Phys. Rev. Lett. **106**, 092001 (2011).
[21] S. Catani, B. R. Webber, and G. Marchesini, Nucl. Phys. **B349**, 635 (1991).
[22] J. André and T. Sjöstrand, Phys. Rev. D **57**, 5767 (1998).
[23] T. Sjöstrand, Phys. Lett. **157B**, 321 (1985).
[24] B. Webber, Annu. Rev. Nucl. Part. Sci. **36**, 253 (1986).
[25] S. Catani and M. Grazzini, Phys. Rev. Lett. **98**, 222002 (2007); S. Catani, L. Cieri, G. Ferrera, D. de Florian, and M. Grazzini, Phys. Rev. Lett. **103**, 082001 (2009).
[26] J. Gao, C. S. Li, and H. X. Zhu, Phys. Rev. Lett. **110**, 042001 (2013).
[27] T. Becher and M. Neubert, Eur. Phys. J. C **71**, 1665 (2011).
[28] T. Gehrmann, T. Lubbert, and L. L. Yang, Phys. Rev. Lett. **109**, 242003 (2012); T. Gehrmann, T. Luebbert, and L. L. Yang, J. High Energy Phys. 06 (2014) 155; Transverse parton distribution functions at next-to-next-to-leading-order, *Proc. Sci.*, RADCOR2013 (2013) 011 [arXiv:1401.1222].
[29] S. Catani, L. Cieri, D. de Florian, G. Ferrera, and M. Grazzini, Eur. Phys. J. C **72**, 2195 (2012).
[30] T. Binoth *et al.*, Comput. Phys. Commun. **181**, 1612 (2010); S. Alioli, S. Badger, J. Bellm, B. Biedermann, F. Boudjema *et al.*, Comput. Phys. Commun. **185**, 560 (2014).
[31] T. Gleisberg and F. Krauss, Eur. Phys. J. C **53**, 501 (2008).
[32] K. Hamilton, P. Nason, C. Oleari, and G. Zanderighi, J. High Energy Phys. 05 (2013) 082.
[33] D. Amati, A. Bassetto, M. Ciafaloni, G. Marchesini, and G. Veneziano, Nucl. Phys. **B173**, 429 (1980).
[34] Y. L. Dokshitzer, D. Diakonov, and S. Troian, Report No. SLAC-TRANS-0183, 1978; D. Amati, R. Petronzio, and G. Veneziano, Nucl. Phys. **B146**, 29 (1978); R. K. Ellis, H. Georgi, M. Machacek, H. D. Politzer, and G. G. Ross, Phys. Lett. **78B**, 281 (1978); S. B. Libby and G. F. Sterman, Phys. Lett. **78B**, 618 (1978); A. H. Mueller, Phys. Rev. D **18**, 3705 (1978); Y. L. Dokshitzer, D. Diakonov, and S. I. Troian, Phys. Rep. **58**, 269 (1980).
[35] S. Catani, L. Cieri, D. de Florian, G. Ferrera, and M. Grazzini, Nucl. Phys. **B881**, 414 (2014).
[36] F. Krauss, R. Kuhn, and G. Soff, J. High Energy Phys. 02 (2002) 044.
[37] A. Buckley, arXiv:0809.4638; A. Buckley, J. Butterworth, D. Grellscheid, H. Hoeth, L. Lönnblad, J. Monk, H. Schulz, and F. Siegert, Comput. Phys. Commun. **184**, 2803 (2013).
[38] A. D. Martin, W. J. Stirling, R. S. Thorne, and G. Watt, Eur. Phys. J. C **63**, 189 (2009).
[39] C. Anastasiou, L. J. Dixon, K. Melnikov, and F. Petriello, Phys. Rev. Lett. **91**, 182002 (2003); Phys. Rev. D **69**, 094008 (2004).
[40] R. Gavin, Y. Li, F. Petriello, and S. Quackenbush, Comput. Phys. Commun. **182**, 2388 (2011); **184**, 208 (2013); Y. Li and F. Petriello, Phys. Rev. D **86**, 094034 (2012).
[41] M. Schönherr and F. Krauss, J. High Energy Phys. 12 (2008) 018.
[42] S. Chatrchyan *et al.* (CMS Collaboration), Phys. Rev. D **85**, 032002 (2012).
[43] G. Aad *et al.* (ATLAS Collaboration), Phys. Lett. B **705**, 415 (2011).
[44] J. Alwall *et al.*, Comput. Phys. Commun. **176**, 300 (2007); J. Butterworth, G. Dissertori, S. Dittmaier, D. de Florian, N. Glover *et al.*, arXiv:1405.1067.
[45] R. Brun and F. Rademakers, Nucl. Instrum. Methods Phys. Res., Sect. A **389**, 81 (1997); Z. Bern, L. J. Dixon, F. Febres Cordero, S. Höche, H. Ita, D. A. Kosower, and D. Maître, Comput. Phys. Commun. **185**, 1443 (2014).